Accepted Manuscript

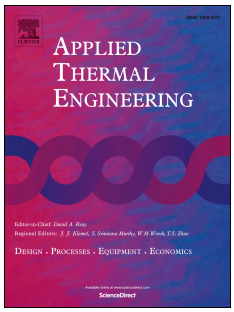

Improved Radial Heat Sink For Led Lamp Cooling

Vítor A.F. Costa , António M.G. Lopes

PII: S1359-4311(14)00332-9

DOI: 10.1016/j.applthermaleng.2014.04.068

Reference: ATE 5592

To appear in: *Applied Thermal Engineering*

Received Date: 9 July 2013

Accepted Date: 25 April 2014

Please cite this article as: V.A.F. Costa, A.M.G. Lopes, Improved Radial Heat Sink For Led Lamp Cooling, *Applied Thermal Engineering* (2014), doi: 10.1016/j.applthermaleng.2014.04.068.

IMPROVED RADIAL HEAT SINK FOR LED LAMP COOLING

Vítor A. F. Costa[1], António M. G. Lopes[2]

1 - Departamento de Engenharia Mecânica, Universidade de Aveiro, Campus Universitário de Santiago, 3810-193 Aveiro, Portugal

2 - ADAI-LAETA, Departamento de Engenharia Mecânica, Universidade de Coimbra 3030-788 Coimbra, Portugal

Abstract

This paper presents a numerical study concerning an improved heat sink for a light emitting diodes (LED) lamp operating under natural convection conditions. Basic geometry of the heat sink is of cylindrical nature, to be obtained from cutting a aluminium extruded bar comprising a cylindrical central core and a number of uniformly distributed radial fins. Minimum diameter of the central core is fixed and the parameters to be explored are the number of fins, their thickness, length (radial dimension) and height. Although not included in the numerical simulations, the thermal resistance due to the use of a thin thermal interface material (TIM) layer between the LED lamp back and the heat sink is taken into account in the analysis. The main objective of the heat sink is to cool the LED lamp so that the lamp maximum temperature at the contact region with the heat sink is maintained below the critical temperature given by the manufacturer. This is a crucial aspect in what concerns the expected lifetime of the LED lamp and should be achieved at the expenses of a as low as possible aluminium mass. Taking these criteria in mind, a design procedure is proposed and followed in the search for the improved heat sink to cool a particular LED lamp. Results obtained with the commercial code ANSYS-CFX clearly show the relative importance of the different governing parameters on the heat sink performance and allow the choice of the better solution within the frame of dimensional constrains. Although the present results concern a particular LED lamp, the proposed methodology can be extended to other types of heat sinks for general light and/or electronic components.

Keywords: LED lamps, heat sink, thermal performance, natural convection heat transfer, conjugate heat transfer

Nomenclature

c_P constant pressure specific heat [J/(kg.ºC)] g gravitational acceleration [m/s^2]

H fin height [m]

H_c height of calculation domain [m]

i number of project variable [-]

k thermal conductivity [W/(m.ºC)]

L fin length, including central core [m]

L_c radius of calculation domain [m]

M heat sink mass [kg]

n number of fins [-]

p pressure [Pa]

Pr Prandtl number [-]

$\dot{Q}$ heat flow [W]

r central core radius [m]

R Thermal resistance [ºC/W]

Ra Rayleigh number [-]

t fin thickness [m]

T temperature [ºC]

u, v, w Cartesian velocity components [m/s]

x, y, z Cartesian coordinates [m]

X_i Generic project variable

Greek symbols

α thermal diffusivity [m^2/s]

β volumetric expansion coefficient [1/K]

Δ difference value

δ thickness of the TIM layer [m]

θ slice angle for calculation domain [rad]

ρ density [kg/m^3]

μ dynamic viscosity [kg/(m.s)]

ν kinematic viscosity [m^2/s]

Subscripts

c core

i optimization variable index

r reference

s solid

∞ ambient

1 - INTRODUCTION

In the past few years, LED lamps have been assuming a large role in the illumination market, mainly due to their potential in creating not only light but interesting light environments, associated with low power consumption even when compared with other *energy-saving* lamp types. Still, from the energetic viewpoint, LED lamps have not yet the desirable efficiency, as a considerable amount of energy is released as heat. This tends to increase the temperature of the LED lamps, leading to a decrease of their lifetime. In order to meet the expected long lifetime, LED lamps must operate below a certain temperature threshold, as given by the manufacturer. To ensure this, the heat sink associated to the LED lamps must provide the needed cooling, requiring the minimum mass of the involved material to obtain the heat sink. Additionally, internal electronic circuitry may have to be

activated by cutting the electrical energy to the LED lamp, changing the illumination characteristics, if by any reason some overshoot on the temperature of the LED lamp occurs.

Thus, one may realize that the design of heat sinks used to cool LED lamps is of major importance to ensure their long lifetime. Heat sinks design criteria should contemplate not only their thermal performance, but also the associated manufacturing costs, which are directly related to the total material mass and production processes involved. For the latest criterion, a uniform cross section is desirable as it can be obtained from simple bars obtained by extrusion, followed by a cutting operation.

Heat sinks for LED lamps can operate under natural or forced convection, the first being the preferred ones as neither additional fans nor electric consumption are required. Additionally, noise generation by electric motors and fans is also avoided if natural convection heat sinks are adopted. On the other hand, natural convection heat sinks are thermally less effective, being consequently less compact and heavier, and need a careful design to reach the required thermal performance.

Heat sinks and LED lamps are assembled together using a thin layer of TIM, which, although designed to have a high thermal conductivity, locally increases the thermal resistance of the assembly.

Some studies can be found in the literature concerning the cooling of LED lamps. This can include what happens inside [1,2] or outside the LED module using detailed CFD studies in a steady-state approach, such as in [3-12], some of them including the packing aspects leading to the LED module. More specifically, Luo *et al.* [1] conducted a numerical and experimental study considering the whole set composed by the vapour chamber and a finned heat sink, and Arika *et al.* [2] consider the thermal management of the set composed by an assembly of LED lamps and a finned heat sink. In the work by Ying *at al.* [3], the optimization of the heat sink associated to a high power LED spot lamp is numerically studied. Scheepers and Visser [4] studied the heat management of high power LEDS using heat sinks through a numerical approach, and comparison is made between the detailed thermal model and simpler thermal resistance models. In the work by Christensen and Graham [5], a 3D numerical simulation is presented for an array of high power LED lamps together with a heat sink, and the thermal resistance network is analysed trying to estimate the different contributions for the heat management, in the search of compact LED systems. Chi *et al.* [6] performed the thermal analysis of high power LED lamps and the associated heat sink, using a CFD numerical simulation together with some heat transfer correlations, including radiation heat transfer. By its own turn, in the study by Weng [7] it is shown how a

detailed 3D CFD analysis can improve the thermal performance of LED illumination systems. The study by Yu *et al.* [8] deals with the numerical simulation and optimization of a radial heat sink, with two alternative configurations having a void central part, for LED cooling purposes, concluding that it is impossible to optimize both thermal performance and heat sink mass, the work by Yu *et al.* [9] including also some experimental results for a similar heat sink configuration. Huang *et al.* [10] studied the thermal dynamics of the overall set of a LED fixture including the luminaire, the LED lamps and the heat sink, and Houl *et al*. [13] studied the thermal dynamics of a LED array system wit in line pin fin heat sink. Ha [11] considered the numerical simulation of a high power LED package and extracted the values of the most relevant thermal resistances of the system. Yu *et al.* [12] analysed the effect of radiation heat transfer on the thermal performance of radial heat sinks similar to that considered in [8] and [9]. Studies considering the problem as a simple thermal resistance combination can also be found [14,15]. Some other studies also include the set composed by the LED module, the heat sink and the luminaries, like in [16]. The recent study by Yu *et al*. [12] shows how radiation heat transfer is relevant when analyzing the thermal behaviour of this kind of heat sinks. Agostini *et al.* [16] present a detailed state of the art for high heat flux cooling technologies. In the work by Shyu *et al.* [17], a 270x1W LED array together with a plate fin heat sink in an acrylic housing is experimentally studied. The complete CFD numerical simulation of single-phase active liquid cooling systems, including minichannels for liquid circulation, can be found in [18]. Huang *et al*. [19] very recently proposed a constant power driving control for a 150 W LED luminaire, thus stabilizing the illumination of LED under large temperature variations.

However, in spite of the referred studies, no work was found concerning the heat sinks for the recent 4th generation LED lamps, like the FORTIMO lamps produced by Philips, more specifically when using a radial heat sink with a central core, obtained by simple extrusion and cutting manufacturing processes. Even if the heat sink by itself is not an energy saving device, it is crucial for the right operation during the expected long lifetime of the energy saving devices that are the LED lamps, and is a relevant applied thermal engineering problem.

The main objective of the present work is to find the improved geometrical configuration for an aluminium heat sink to be used in 4th generation FORTIMO LED lamps, given the heat release rate, critical (maximum) temperature of the LED module and space constraints. The improved configuration is, in the present context, that corresponding to the lowest heat sink mass that guarantees the required cooling level. Any economic analysis, even if requiring reliable information which may be difficult to obtain, will lead coincidently to the cheaper heat sink, obtained from the lowest mass of material and requiring the simplest manufacturing processes to obtain it. The

procedure proposed in the present work leads to an improvement path that, starting from an initial guess, is governed by the partial derivatives of the maximum (core) temperature with respect to the heat sink mass, for each geometrical parameter under study. This is different from an integrated optimization procedure, as no special optimization techniques and tools are needed, and the improved heat sink can be obtained by non-experts in optimization studies, following a way with its own physical insight and not as an optimization mathematical problem. Some of the results obtained with the commercial code ANSYS-CFX during the improvement process are presented, along with the final solution corresponding to the founded improved effective heat sink.

2 - PHYSICAL MODELING

As the heat sink is considered in the vertical position, as presented in Fig. 1, relatively cold ambient air approaches the hot heat sink and becomes warmer, thus rising and pulling new fresh air from the colder ambient to satisfy continuity. The resulting flow assumes the form of a rising plume, air entering the heat sink in an essentially radial (horizontal) direction and leaving it in an essentially vertical direction. Heat sink remains warm due to the heat released by the LED lamps assembly, the manufacturer of the LED lamp giving the value of the heat released to the heat sink, which needs to be released by the heat sink to the natural convection air flow. The balance between the heat released by the LED lamp to the heat sink and the heat released by the heat sink to the cooling air dictates the temperature at the centre (core) of the LED lamp module, which needs to be below a critical temperature value specified by the LED lamp manufacturer. More effective heat sinks lead to lower temperatures at the centre of the LED lamp module, the best heat sink being that allowing a temperature at the center of the LED lamp module close to the critical value given by the LED lamp manufacturer but requiring the lowest mass of material to obtain it.

2.1 - Physical model

The heat sink to be studied is radial, with a circular base and a number of equally spaced rectangular fins joining at a central core. The heat sink seats on the top (back) of the LED module, as depicted in Figure 1a). The recent FORTIMO DLM GEN 4 3000/830 LED module considered in this work features a rectangular base releasing the maximum thermal power of 19.2 W through the 8.3×7.8 cm^2 rectangular base. The manufacturer advises a maximum temperature at the LED base below 70 ºC, when operating under an ambient air temperature of 35 ºC.

The adopted heat sink starting configuration for the improvement process (basic configuration) has a base diameter similar to the LED module largest diagonal, thus ensuring full contact with the

heat sink at LED module base. Table 1 presents the physical dimensions according to the schematic drawing in Figure 1b). The considered heat sink includes a thin aluminium disk between the back of the LED module and the main body of the heat sink, mainly for fixing purposes. However, other solutions including screws acting over the fins themselves can be designed for that purpose.

2.2 - Governing equations

Natural convection is governed by the Prandtl number:

$$Pr = \frac{\nu}{\alpha} \tag{1}$$

and by the Rayleigh number:

$$Ra = \frac{g\,\beta\,\Delta T\,L_r^{\,3}}{\nu^2}\,Pr \tag{2}$$

where all properties refer the air involving the heat sink.

For the present case, taking the reference length L_r as the heat sink base diameter and the representative temperature difference between the heat sink and ambient air as $\Delta T \approx 40^{\circ}\mathrm{C}$, Eq. (2) computes $Ra \approx 6\times10^{6}$, which is well below the typical transition value 10^{8}-10^{9} for the turbulent regime [20]. Therefore, laminar conditions are assumed, corresponding to a conjugate laminar natural convection 3D problem in steady-state conditions.

Warming up and cooling down periods of LED lamps are considerably short when compared with the continuous longer and nearly steady operating periods, thus justifying that only the steady state operation conditions are considered in the present work. Governing equations are the mass conservation equation, the momentum (Navier-Stokes) equations and the thermal energy conservation equation, which read, respectively:

$$\frac{\partial}{\partial x}(\rho u)+\frac{\partial}{\partial y}(\rho v)+\frac{\partial}{\partial z}(\rho w)=0 \tag{3}$$

$$\frac{\partial}{\partial x}(\rho uu)+\frac{\partial}{\partial y}(\rho vu)+\frac{\partial}{\partial z}(\rho wu)=-\frac{\partial p}{\partial x}+\mu\left(\frac{\partial^2 u}{\partial x^2}+\frac{\partial^2 u}{\partial y^2}+\frac{\partial^2 u}{\partial z^2}\right) \tag{4a}$$

$$\frac{\partial}{\partial x}(\rho uv)+\frac{\partial}{\partial y}(\rho vv)+\frac{\partial}{\partial z}(\rho wv)=-\frac{\partial p}{\partial y}+\mu\left(\frac{\partial^2 v}{\partial x^2}+\frac{\partial^2 v}{\partial y^2}+\frac{\partial^2 v}{\partial z^2}\right) \tag{4b}$$

$$\frac{\partial}{\partial x}(\rho uw)+\frac{\partial}{\partial y}(\rho vw)+\frac{\partial}{\partial z}(\rho ww)=-\frac{\partial p}{\partial z}+\mu\left(\frac{\partial^2 w}{\partial x^2}+\frac{\partial^2 w}{\partial y^2}+\frac{\partial^2 w}{\partial z^2}\right)-\rho g \tag{4c}$$

$$\frac{\partial}{\partial x}(\rho uT)+\frac{\partial}{\partial y}(\rho vT)+\frac{\partial}{\partial z}(\rho wT)=\frac{k}{c_P}\left(\frac{\partial^2 T}{\partial x^2}+\frac{\partial^2 T}{\partial y^2}+\frac{\partial^2 T}{\partial z^2}\right) \quad (1)(5)$$

where the work of pressure forces and viscous dissipation were neglected in the thermal energy conservation equation. Within the solid, advection terms vanish, leading to the heat conduction equation:

$$0=\frac{\partial}{\partial x}\left(k_s\frac{\partial T}{\partial x}\right)+\frac{\partial}{\partial y}\left(k_s\frac{\partial T}{\partial y}\right)+\frac{\partial}{\partial z}\left(k_s\frac{\partial T}{\partial z}\right) \quad (6)$$

In the previous equations, fluid and solid properties were considered as constant, expect for fluid density in the buoyancy term on the *z* momentum equation, which is computed based on the Ideal Gas Law.

Due to the expected temperature differences between solid surfaces and the environment and physical proximity between the solid surfaces, heat transfer by radiation must be taken into account. It represents an additional heat transfer mode promoting heat transfer from the base of the heat sink to its fins, and thus increases the effectiveness of the heat sink. Several models exist to consider the surface radiation heat transfer in the numerical model, with specific capabilities depending on the physical problem under analysis. In the present case, due to the transparent nature of the air, the Monte Carlo radiation model represents the best option [21]. This model simulates the interaction between photons and the environment, a process that is carried out by following the path of a predetermined number of photons, including surface reflection, absorption and scattering, and it is one of the radiation model options included in the ANSYS-CFX software package.

2.3 - Computational model and boundary conditions

ANSYS-CFX software package is a well-known and well-established software package, which has been used and validated under many different conditions, and also to solve natural convection problems. As a certified software, extensive validation has been done by different research groups under a great variety of situations, with corresponding documentation available through the internet and in different reports available from ANSYS, including both laminar and turbulent flows [22], as well as free convection with conjugate heat transfer [23]. CFX uses a coupled solver in a co-located (non-staggered) mesh. In order to avoid the well know checkerboard pressure field, a fourth-order Rhie- Chow interpolation scheme is used. In the present simulations, advection terms were modelled using the CFX-high resolution scheme option, which ensures boundness of the solution. A trilinear interpolation scheme was adopted for the evaluation of the diffusion terms and pressure gradient As based on a finite volume formulation, discretization equations, and in particular the

enthalpy (thermal energy) equations, are obtained for each control volume. Boundaries between fluid and solid domains coincide with control volume faces at these locations, and no boundary conditions need to be specified as a normal conservative condition is considered. Thus, the obtained discretized equations for enthalpy ensure thermal energy conservation in the fluid-solid interface, the conjugate heat transfer being *automatically* taken into account through this integration approach.

For the sake of simulations, the physical presence of the LED module was not taken into account. This leads to a geometry that possesses a periodic angular behaviour, allowing the simulations to be carried out for a single fin. Placement of computational domain boundaries and mesh size were carefully chosen so as to guarantee results' independence on both mesh and calculation domain. On the other hand, corresponding values such as number of mesh nodes and domain dimensions were tested in order to keep computer requirements at reasonable levels. Figure 2a shows the computational domain geometry adopted for the simulations, for which $L_c = 0.13\,\text{m}$ and $H_c = 0.09\,\text{m}$. Different mesh sizes were tested as well, leading to a solution characterized by a total of about 200,000 nodes (cf. Figure 2b), using a target inner mesh size in the air domain of 0.002 m. In the air-solid interface, where typical mesh elements size is 0.0005 m, an inflated layer 2×10^{-5} m high with prismatic elements was employed so as to better simulate the heat transfer mechanism therein.

For the solid domain, the heat flux value was imposed at the bottom boundary (heat sink base), so as to satisfy a total of 19.2 W (the heat flow released by the LED array). Lateral boundaries of the calculation domain were assigned an angular periodic condition, while non-slip conditions were applied at all the solid-gas interfaces. For the gas domain, besides the angular periodicity applied to the corresponding boundaries, an open-type condition with zero relative pressure and 35 ºC temperature was considered for all the exterior boundaries. Inlet velocities at the different portions of the external boundaries are thus obtained as that required by the natural convection problem under analysis. If part of an exterior boundary is an outlet for fluid a parabolic exit boundary condition is considered there. The solid-gas interfaces are treated with an energy-conservative condition, which is automatically taken into account as the numerical method is based on a control volume approach. For radiation calculations, aluminium surfaces are assumed as gray with diffusive reflection, featuring an emissivity of 0.85. A total of 10,000 photons was used for the application of the Monte Carlo Model, considering a surrounding temperature of 35 ºC.

Obtained results qualitatively agree with results for similar LED lamp modules obtained from the literature, and no exhaustive comparison can be made as no other numerical or experimental results are known for the FORTIMO DLM GEN 4 3000/830 LED module.

2.4 - Thermal resistance at the LED module-heat sink contact

The attachment between the aluminium heat sink and the LED module is made with screws. In order to reduce the thermal resistance between both solids, a TIM is commonly used, so that no air gaps due to surface roughness are present in the interface to considerably increase the contact thermal resistance.

The temperature drop at the contact interface may be easily computed using a simple 1D analysis. The governing heat conduction equation is:

$$\dot{Q} = k\, A_c \frac{\Delta T_i}{\delta} \quad \Rightarrow \quad \Delta T_i = \frac{\dot{Q}\,\delta}{k\, A_c} \tag{7}$$

The thermal conductivity of a good TIM material, like DOW CORNING TC-5022, is typically 4 W/(m ºC). Considering a film thickness of 0.0002 m, the total heat release rate, and heat sink base area as presented previously, an interface temperature drop $\Delta T_i = 0.077\ ^\circ\mathrm{C}$ is obtained from Eq. (7). Therefore, one may conclude that the additional temperature drop due to the contact resistance can be neglected in subsequent analysis. However, if this temperature drop is not so low, and if it is to be considered, the one dimensional analysis is followed through the thin TIM layer and the numerical domain refers only to the solid aluminium body of the heat sink, the maximum admissible temperature at the heat sink being the maximum temperature admissible at the LED module minus the temperature drop through the TIM layer. Even so, to accommodate any uncertainty on the calculations, as well as the negative effects on cooling of some dirty that can accumulate over the surfaces of the heat sink, a maximum core temperature of 65 ºC was taken as the objective in this study.

3 - IMPROVEMENT STRATEGY

As previously pointed out, the objective of the present work is to obtain the improved heat sink geometrical configuration so as to guarantee that the LED module maximum temperature value (verified at the LED module base) is below the manufacturer threshold. This is to be achieved with a as low as possible heat sink mass, provided the geometrical dimensions are kept within reasonable limits. It is anticipated that an increase on the thickness of the fins, and increase on the length of the fins, and an increase on the height of the heat sink will result on an increased thermal effectiveness

of the heat sink. It is also anticipated that an increase on the number of fins will result in an increase on the thermal effectiveness of the heat sink below a given number of fins, but that this behaviour is inverted above that given number of fins, as a high number of fins results in a smaller and narrower available space for the natural convection risen flow. However, the increase of any of the referred parameters will result on an increase of the mass needed to obtain the heat sink, and it needs to be evaluated what is the parameter to be increased resulting in the higher increase on the thermal effectiveness of the heat and simultaneously to the lower increase on the mass needed to obtain the heat sink. This is the criterion to be followed when searching for an improved heat sink to cool the particular LED lamps assembly considered, starting from a given non-optimal initial heat sink geometry.

The geometry parameterization was set according to the project variables listed in Table 1: fin height *H*, fin thickness *t*, fin length *L* and number of fins, *n*. The core minimum radius r_1, also listed in this table, is kept constant. The maximum temperature T_c (core temperature) to be evaluated at the base of the heat sink (as referred, due to its small value, the temperature drop across the TIM material is neglected), is a function of these variables:

$$T_c = T_c\left(X_i\right), \quad i = 1,2,3,4; \ \left(X_i = H, t, L, n\right) \tag{8}$$

A change ΔX_i of one of the project variables X_i will lead to a change in both the core temperature ΔT_{ci} and the heat sink mass ΔM_i:

$$\Delta T_{ci} = \frac{\partial T_{ci}}{\partial X_i}\Delta X_i \quad ; \quad \Delta M_i = \frac{\partial M_i}{\partial X_i}\Delta X_i \tag{9}$$

It can be easily seen that, attending to the definition of each project variable, increasing any of the project variables will lead to a mass increase – any of the partial mass derivative in the previous equation is always positive and can be analytically calculated. On the other hand, the core temperature partial derivatives must be evaluated through simulation and their sign is most often negative (except, as will be seen, for $\partial T / \partial n$ at large values of *n*). Therefore, one may realize that, since the improvement path to follow should be evaluated in terms of both mass and core temperature variations, the governing variable is $\partial T_{ci} / \partial M_i$, which is negative in the improvement space – decreasing the core temperature is achieved at the expenses of an increase of the heat sink mass.

The improvement path criterion will thus be:

- Improvement variables *i* with a large value $\left|\partial T_{ci} / \partial M_i\right|$ should be changed towards a mass increase, in order to achieve a "large" core temperature decrease at the expenses of "small" mass increase ;

- Improvement variables *i* with a small value $\left|\partial T_{ci} / \partial M_i\right|$ should be changed towards a mass decrease, in order to decrease heat sink mass at the expenses of only a small core temperature increase.

Based on the previous considerations, the improvement strategy is:

- Starting with the basic configuration (cf. Table 1), evaluate the absolute value of the partial derivatives $\left|\partial T_{ci} / \partial M_i\right|$ through numerical simulation, by changing, in turn, each improvement parameter and using the obtained values for T_c and M readily available in the software post-processor.

- Identify the improvement parameter(s) with the largest $\left|\partial T_{ci} / \partial M_i\right|$ value and proceed the improvement towards lower T_c values, taking also into account geometry constraints. In this sense, the number of fins n will be a priority as this improvement parameter doesn´t influence the total occupied volume; on the other hand, fin length L and height H should be kept at the admissible minimum values.

- Fine tune the improvement, by checking the heat sink dimensions and decreasing the heat sink mass using improvement variable(s) with low $\left|\partial T_{ci} / \partial M_i\right|$.

4 - RESULTS AND ANALYSIS

The starting point for the improvement process is the basic configuration detailed in Table 1, for which numerical computations led to a core temperature $T_c = 87.65\,^{\circ}\mathrm{C}$ and a heat sink mass $M = 0.197$ kg. For the heat sink thermal resistance based on the maximum core temperature, given by

$$R = \frac{T_c - T_\infty}{\dot{Q}_i} \tag{10}$$

a value of 2.742 ºC/W was obtained. These results are synthesized in Table 2. Figure 3 depicts a visualization of the results for: (a) The velocity field at a vertical plane located between two fins; and (b) The temperature field at the heat sink. The difference between the heat sink temperature and

the ambient air temperature creates buoyancy forces that produce an ascending air movement towards the heat sink core. As the air mass passes between the fins, its temperature increases, creating a higher temperature region in the plume central part, as it is well illustrated by the temperature coloured vectors in Figure 3. The temperature range at the solid domain is only about 0.8 ºC, due to the considerably high thermal conductivity of the aluminium; even so, as expected, temperatures at the heat sink core are higher than those at the exposed part of the fin.

Table 3 lists the adopted data for the initial variation of the improvement parameters, necessary for the evaluation of the partial derivatives of core temperature with respect to the mass of the heat sink. As expected, fin length is the parameter with the largest influence in the core temperature. Although these results would point out a fin length increase as the best choice to proceed to improve the heat sink, the total occupied volume would also increase by a large amount, since for the basic configuration the fins already protrude outside the heat sink base. As pointed out previously, the number of fins should be a priority parameter since the total occupied volume is not affected when changing this parameter. Dependence of the core temperature and $\partial T_{ci} / \partial M_i$ with this parameter is shown in Figure 4. It is interesting to observe the evolution of these variables with *n*, revealing that the effectiveness of adding more fins vanishes as the number of fins increases. This is a consequence of the small spacing between each two adjacent fins, which prevents fresh air to penetrate the inter-fin space and remove heat from there, decreasing the overall heat sink effectiveness. It is, therefore, not advisable to choose a too large number of fins.

Based on these results, a maximum of 40 fins was established, corresponding to a core temperature $T_c = 72.85\,^{\circ}\mathrm{C}$ and to a heat sink mass $M = 0.316$ kg.

Analysing the partial derivatives presented in Table 3, one may note that a fin thickness change will allow reducing mass without a significant core temperature increase. Accordingly, as a next step, fin thickness was reduced from 2 mm (basic configuration) to 1 mm, from which a core temperature $T_c = 73.47\,^{\circ}\mathrm{C}$ and a heat sink mass $M = 0.197$ kg were obtained, for *n* = 40 fins. It is interesting to check that, with this reduced fin thickness, the dependence of T_c with *n* became larger and the inversion of the $\partial T_{ci} / \partial M_i$ sign was not found up to *n* = 70, as shown in Figure 5. By increasing the number of fins and reducing their thickness, one could reduce the core temperature by approximately 14 ºC and the thermal resistance by 27%, for a total mass similar to the initial configuration.

Further reduction from $T_c = 73.47\,^{\circ}\mathrm{C}$ to values below 70 ºC can be achieved by increasing the fin height. Simulation results are as depicted in Figure 6 and in Table 4. From a simple linear interpolation, one could anticipate a value $H = 0.028\,\mathrm{m}$ necessary for $T_c = 65\,^{\circ}\mathrm{C}$, which was confirmed with the numerical simulation, corresponding to a heat sink mass $M = 0.244\,\mathrm{kg}$. The final configuration for the heat sink is depicted in Figure 7, along with the visualization of the obtained temperature field at the heat sink surface.

One may then conclude that, starting from an original heat sink configuration with mass 0.197kg leading to a core temperature $T_c = 87.65\,^{\circ}\mathrm{C}$ and thermal resistance $R = 2.742$ ºC/W, the proposed improvement allowed a reduction of $22.65\,^{\circ}\mathrm{C}$ in the core temperature to reach $T_c = 65\,^{\circ}\mathrm{C}$, for a final thermal resistance $R = 1.281$ ºC/W. This was achieved at the expenses of a mass increase of only 24%, corresponding to a final mass $M = 0.244\,\mathrm{kg}$. It must be retained that this is the improved solution, which satisfactorily provides the required cooling for the considered LED lamp involving a satisfactory mass of aluminium, but that it is not the optimum solution in a strict sense, and that even slightly better solutions can be obtained through the finest tuning of the governing parameters, following the described improvement strategy.

The results presented and discussed in the present work are specific for the FORTIMO DLM GEN 4 3000/830 LED module. However, attending that improved or even optimum cooling systems may be needed for other LED lamp modules, the used methodology, with its own physical insight and without requiring knowledge and use of optimization tools and software, can and must be used when searching for the best cooling system for other LED lamp modules.

5 - CONCLUSIONS

An improvement procedure was presented and followed to find the improved geometrical configuration for a heat sink operating under natural convection conditions, to be used for the cooling of a recent FORTIMO 4th generation LED lamp. The objective was to achieve a maximum core temperature of 65 ºC keeping the heat sink total mass and occupied volume contained. Numerical simulations were done for conjugate laminar steady state natural convection, including heat transfer by radiation through the Monte Carlo model. The improvement path is given by the partial derivatives of the core temperature with respect to the mass of the heat sink, subjected to occupied volume constraints. Improvement variables considered were number of fins, fin height, fin length and fin thickness. Starting from a basic configuration leading to a core temperature $22.65\,^{\circ}\mathrm{C}$ above the required limit, the objective core temperature of $65\,^{\circ}\mathrm{C}$ was reached by increasing the

number of fins and their height and reducing the fin thickness. These geometrical modifications were responsible for a heat sink mass increase of only 0.047 kg, which represents approximately 24% of the initial mass, but to a considerable temperature decrease, up to reach the admissible maximum core temperature of the LED module.

The presented methodology is general in character and may be extended to improve other types of heat sinks for virtually any light and/or electronic components.

6 - REFERENCES

1. X. Luo, R. Hu, T. Guo, X. Zhu, W. Chen, Z. Mao, S. Liu, Low thermal resistance LED light source with vapor chamber coupled fin heat sink, *IEEE 2010 Electronic Components and Technology Conference*, Paris, Las Vegas, 2010 (doi: 10.1109/ECTC.2010.5490645).
2. M. Arika, C. Beckerb, S. Weaverb, J. Petroskic, Thermal management of LEDs: package to system, *Third International Conference on Solid State Lighting SPIE*, Bellingham, WA, 2004, *Vol. 5187* (doi: 10.1117/12.512731).
3. Y. G.-Ying, Z. X. Ping, H. S.-Hong, H. W-Wen, G. T.-Tai, Thermal simulation and optimization design on a high power LED spot lamp, *Optoelectronics Letters* 7 (2) (2011) 117-121 (doi: 10.1007/s11801-011-0142-8).
4. G. Scheepers, J. A. Visser, Detailed thermal modeling of high powered LEDs, *25th IEEE SEMI-THERM Symposium 2009*, San José, California, 2009 (doi: 10.1109/STHERM.2009.4810747).
5. A. Christensen, S. Graham, Thermal effects in packaging high power light emitting diode arrays, *Applied Thermal Engineering* 29 (2009) 364–371 (doi: 10.1016/j.applthermaleng.2008.03.019).
6. W.-H. Chi, T.-L. Chou, C.-N. Han, K.-N. Chiang, Analysis of thermal performance of high power light emitting diodes package, *IEEE 2008 10th Electronics Packaging Technology Conference*, Singapore, 2008 (doi: 10.1109/EPTC.2008.4763488).
7. C.-J. Weng, Advanced thermal enhancement and management of LED packages, *International Communications in Heat and Mass Transfer* 36 (2009) 245–248 (doi: 10.1016/j.icheatmasstransfer.2008.11.015).
8. S.-H. Yu, K.-S. Lee, S.-J. Yook, Optimum design of a radial heat sink under natural convection, *International Journal of Heat and Mass Transfer* 54 (2011) 2499–2505 (doi: 10.1016/j.ijheatmasstransfer.2011.02.012).

9. S.-H. Yu, K.-S. Lee, S.-J. Yook, Natural convection around a radial heat sink, *International Journal of Heat and Mass Transfer* 53 (2010) 2935–2938 (doi: 10.1016/j.ijheatmasstransfer.2010.02.032).

10. B.-J. Huang, C.-W. Tang, M.-S. Wu, System dynamics model of high-power LED luminaire, *Applied Thermal Engineering* 29 (2009) 609–616 (doi: 10.1016/j.applthermaleng.2008.03.038).

11. M. S. Ha, *Thermal Analysis of High Power LED Arrays*, MSc. Thesis, School of Mechanical Engineering, Georgia Institute of Technology, Atlanta, GA, 2009.

12. S.-H. Yu, D. Jang, K.-S. Lee, Effect of radiation in a radial heat sink under natural convection, *International Journal of Heat and Mass Transfer* 55 (2012) 505–509 (doi: 10.1016/j.ijheatmasstransfer.2011.09.026).

13. F. Houl, D. Yangl, G. Q. Zhangl, Y. Hail, D. Liul, L. Liul, Thermal transient analysis of LED array system with in-line pin fin heat sink, *12th. Int. Conf. on Thermal, Mechanical and Multiphysics Simulation and Experiments in Microelectronics and Microsystems, IEEE EuroSimE 2011*, Linz, Austria, 2011 (doi: 10.1109/ESIME.2011.5765844).

14. X. Luo, W. Xiong, S. Liu, A simplified thermal resistance network model for high power LED street lamp, *IEEE International Conference on Electronic Packaging Technology & High Density Packaging (ICEPT-HDP 2008)*, Shangai, China, 2008 (doi: 10.1109/ICEPT.2008.4606976).

15. X. Luo, W. Xiong, T. Cheng, S. Liu, Design and optimization of horizontally-located plate fin heat sink for high power LED street lamps, *2009 IEEE Electronic Components and Technology Conference* (2009) 854-859, San Diego, California, 2009 (doi: 10.1109/ECTC.2009.5074112).

16. B. Agostini, M. Fabbri, J. E. Park, L. Wojtan, J. R. Thome, B. Michel, State of the art of high heat flux cooling technologies, *Heat Transfer Engineering* 28(4) (2007) 258–281 (doi: 10.1080/01457630601117799).

17. B. J.-C. Shyu, K.-W. Hsu, K.-S. Yang, C.-C. Wang, Thermal characterization of shrouded plate fin array on an LED backlight panel, *Applied Thermal Engineering* 31 (2011) 2909-2915 (doi: 10.1016/j.applthermaleng.2011.05.019).

18. B. Ramos-Alvarado, B. Feng, G. P. Peterson, Comparison and optimization of single-phase liquid cooling devices for the heat dissipation of high-power LED arrays, *Applied Thermal Engineering* 59 (2013) 648-659 (doi: 10.1016/j.applthermaleng.2013.06.036).

19. B.-J. Huang, C.-W. Chen, C.-D. Ong, B.-H. Du, P.-C. Hsu, Development of constant-power driving control for light-emitting-diode (LED) luminaire, *Applied Thermal Engineering* 50 (2013) 645-651 (doi: 10.1016/j.applthermaleng.2012.07.030).

20. A. Bejan, *Heat Transfer*, Wiley, New York, 1993.

21. M. Modest, *Radiation Heat Transfer*, McGraw-Hill, New York, 1993.

22. W. Vieser, T. Esch, F. Menter, Heat transfer predictions using advanced two-equation turbulence models, ANSYS CFX Validation Report, CFX-VAL10/0404, ANSYS Europe Ltd., 2002.

23. H. Xu, C. Guetari, K. Svihla, Simulation of free convection with conjugate heat transfer, 2006 International ANSYS Conference: A World of Simulation, Pittsburgh, PA, 2006.

FIGURE CAPTIONS

Figure 1. The heat sink. (a) 3D view of the ensemble; (b) geometrical parameters.

Figure 2. Calculation domain, for a single fin, basic configuration. (a) Domain dimensions; (b) Non-structured mesh.

Figure 3. Results for the basic configuration. (a) Velocity field vectors at the vertical plane between two fins (vectors are coloured according to local temperature); (b) Temperature field at the heat sink surface.

Figure 4. Influence of number of fins, for t = 2 mm. (a) Core temperature versus number of fins; (b) $\partial T_c/\partial M$ versus number of fins.

Figure 5. Influence of number of fins, for t = 1 mm. (a) Core temperature versus number of fins; (b) $\partial T_c/\partial M$ versus number of fins.

Figure 6. Influence of fin height. (a) Core temperature versus fin height; (b) Core temperature versus heat sink mass.

Figure 7. Final configuration for the improved heat sink. (a) Heat sink geometry; (b) Temperature distribution at the heat sink surface.

TABLES

Table 1. Basic geometric configuration of the heat sink.

Core radius r_1	Fin height H	Fin thickness t	Fin length L	N of fins/ Angle n/θ
0.01 m	0.021 m	0.002 m	0.063 m	20/18º

Table 2. Results for basic configuration

Core temperature T_c [ºC]	Thermal Resistance R [ºC /W]	Heat sink mass M [kg]
87.65 ºC	2.742	0.197

Table 3. Variation of optimization parameters for the initial calculation of partial derivatives.

	Fin height H	Fin thickness t	Fin length L	Number of fins n
ΔX_i	0.004 m	-0.001 m	-0.0053 m	5
$\partial T_{ci} / \partial M_i$	-260 ºC/kg	-20 ºC/kg	-800 ºC/kg	-150 ºC/kg

Table 4. Simulation results for changing fin height.

Fin height H [m]	Core temperature T_c [ºC]	Thermal Resistance R [ºC /W]	Heat sink mass M [kg]
0.021	73.5	2.005	0.197
0.025	68.0	1.719	0.223
0.030	63.6	1.49	0.256
0.035	59.6	1.281	0.289

FIGURES

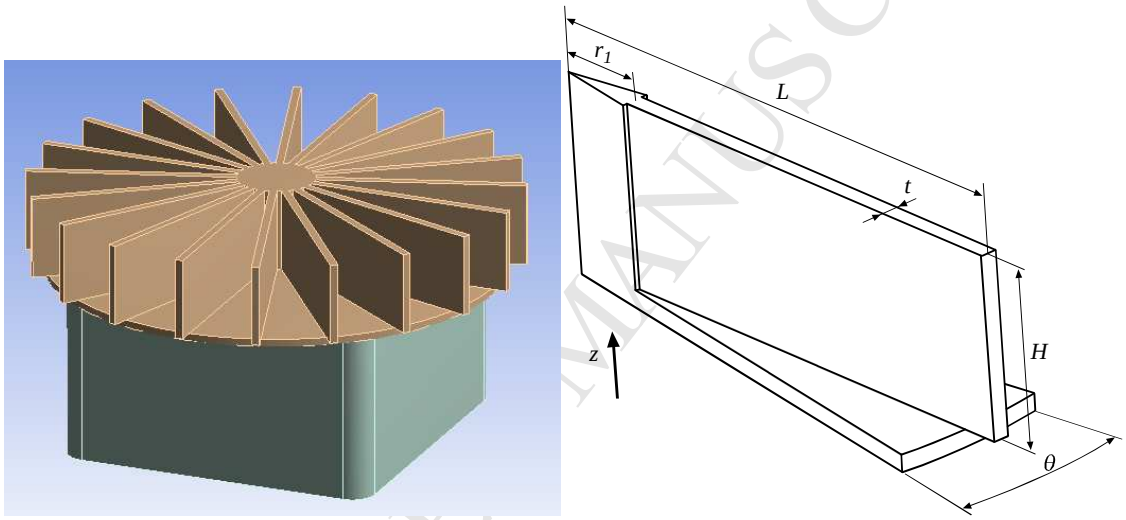

(a) (b)

Figure 1. The heat sink. (a) 3D view of the ensemble; (b) geometrical parameters.

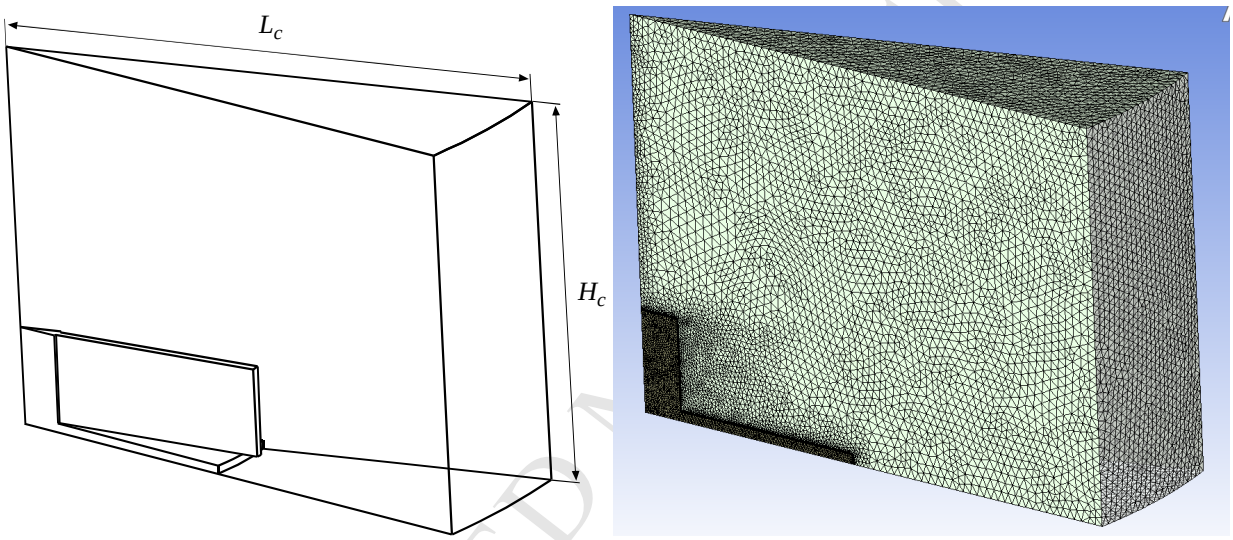

(a) (b)

Figure 2. Calculation domain, for a single fin, basic configuration. (a) domain dimensions. (b) non-structured mesh.

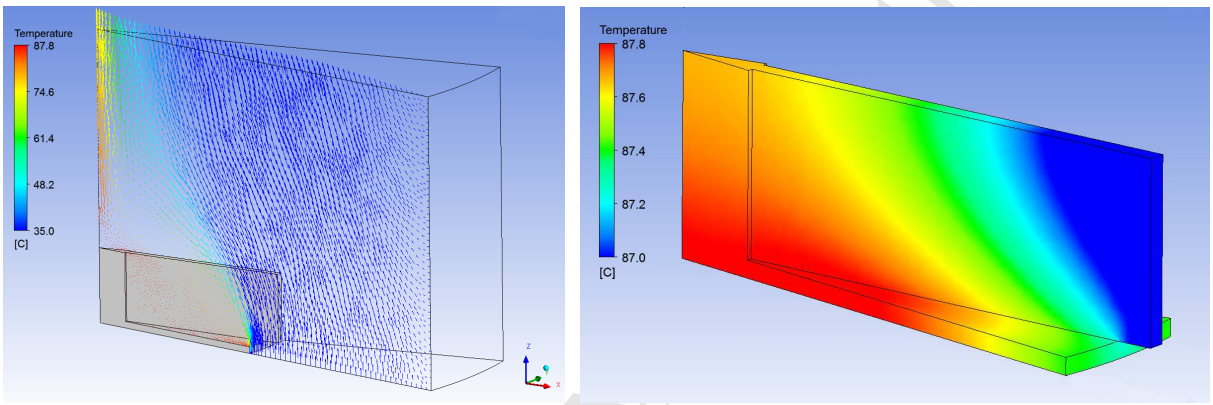

(a) (b)

Figure 3. Results for the basic configuration. (a) Velocity field vectors at the vertical plane between two fins. Vectors are coloured according to local temperature; (b) Temperature field at the heat sink surface.

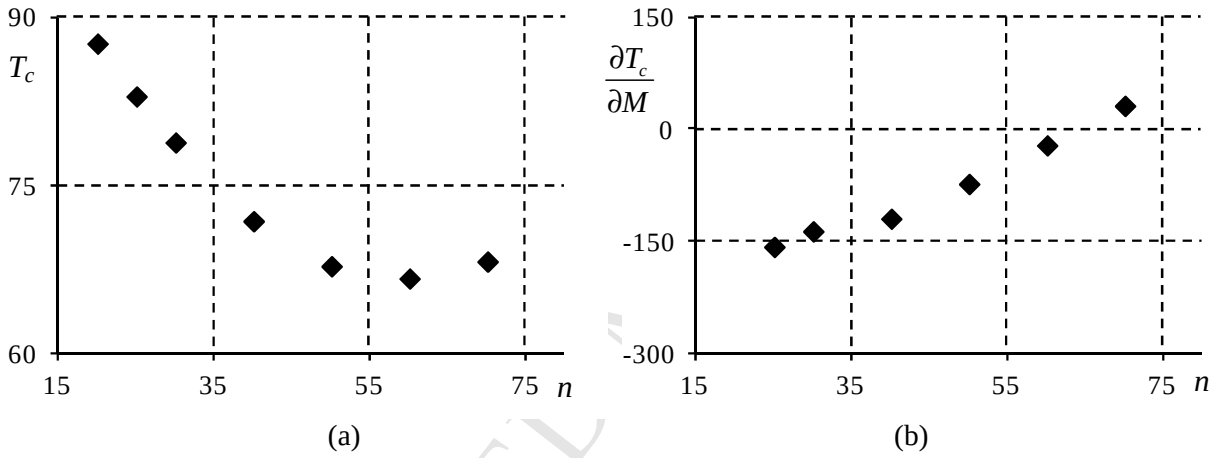

Figure 4. Influence of number of fins, for t = 2 mm. (a) Core temperature versus number of fins; (b) $\partial T_c/\partial M$ versus number of fins.

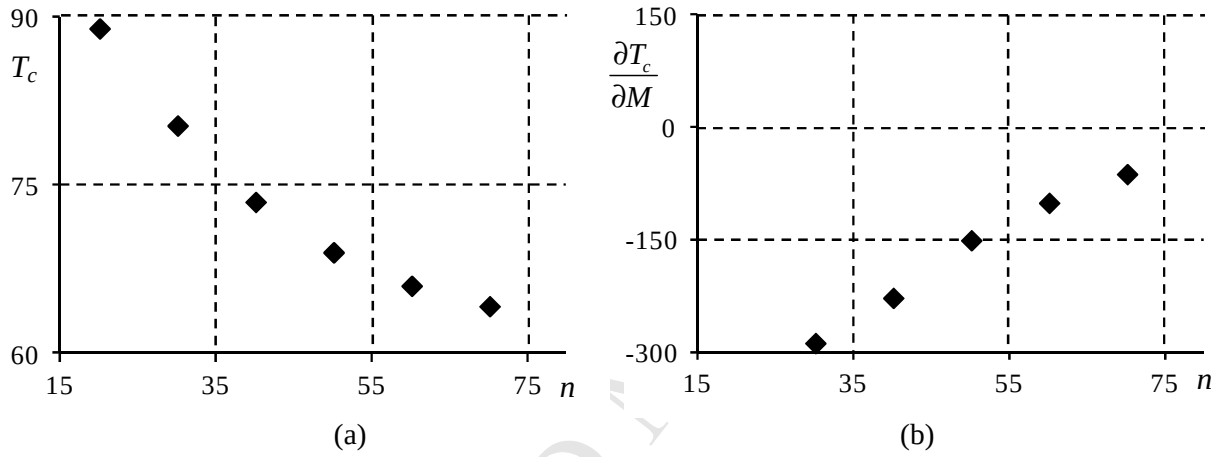

Figure 5. Influence of number of fins, for t = 1 mm. (a) Core temperature versus number of fins; (b) $\partial T_c/\partial M$ versus number of fins.

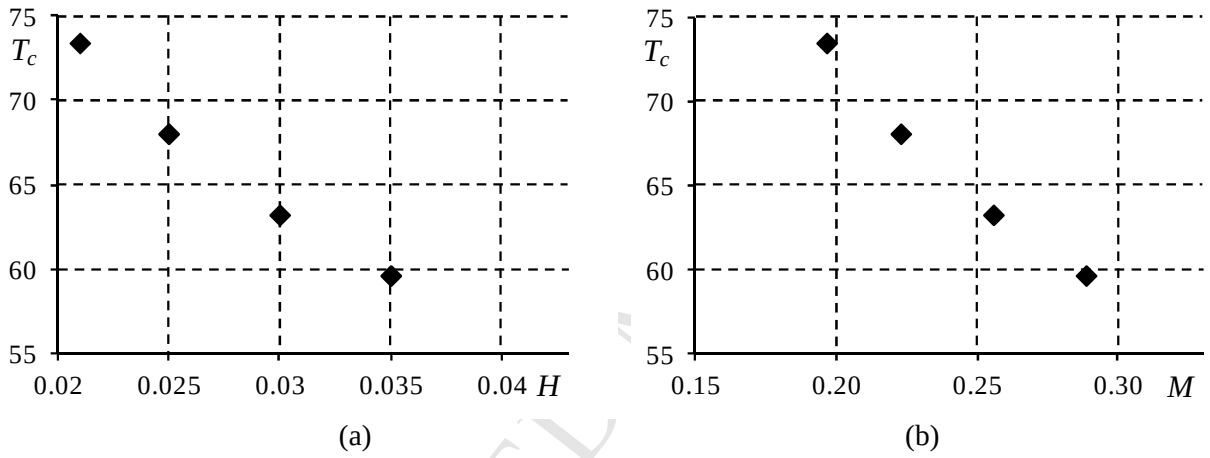

Figure 6. Influence of fin height. (a) Core temperature versus fin height; (b) Core temperature versus heat sink mass.

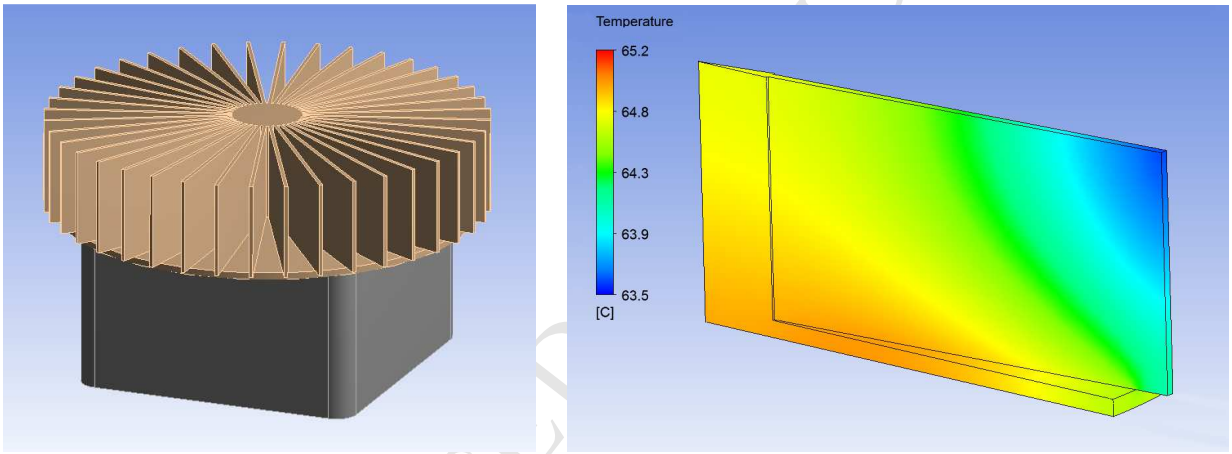

(a) (b)

Figure 7. Final configuration for the improved heat sink. (a) Heat sink geometry; (b) Temperature distribution at the heat sink surface.

IMPROVED RADIAL HEAT SINK FOR LED LAMP COOLING

Vítor A. F. Costa[1], António M. G. Lopes[2]

1 - Departamento de Engenharia Mecânica, Universidade de Aveiro, Campus Universitário de Santiago, 3810-193 Aveiro, Portugal
2 - ADAI-LAETA, Departamento de Engenharia Mecânica, Universidade de Coimbra 3030-788 Coimbra, Portugal

HIGHLIGHTS FOR REVIEW

A numerical study is made concerning the radial heat sink for a specific LED lamp.

The cylindrical heat sink is obtained from an extruded aluminum bar.

The required cooling effect is obtained using the minimum mass of material.